euronoise

Nonlinear pulsing schemes for the detection of ultrasound contrast agents

Michalakis Averkiou[a], Christophoros Mannaris[a], Matthew Bruce[b] and Jeffry Powers[c]

[a]University of Cyprus/Dept. of Mech. Engineering, 75 Kallipoleos Str., 1678 Nicosia, Cyprus
[b]SuperSonic Imagine, Les Jardins de la Duranne - Bât. E, 510, rue René Descartes, F - 13857 Aix-en-Provence, France
[c]Philips Medical Systems, 22100 Bothell Everett Hwy, Bothell, WA 98021, USA
maverk@ucy.ac.cy

Nonlinear imaging techniques have been used in diagnostic ultrasound in tissue harmonic imaging (THI) and in imaging of ultrasound contrast agents (UCAs). While in THI the nonlinearity comes from propagation, in UCAs the nonlinearity comes from the scattering process. Nonlinear pulsing schemes, transmitting a series of pulses and then combining the scattered signals in a way that all linear components cancel, have been proposed and implemented in diagnostic scanners. Various pulsing schemes for the detection of nonlinear echoes from tissues and contrast microbubbles were investigated experimentally in the present work. The pulsing schemes considered were pulse inversion (PI), power modulation (PM), and their combination (PMPI). Emphasis was placed on identifying the unique nonlinear components in the various pulsing schemes and their relative harmonic levels. Experiments of nonlinear propagation in water and nonlinear scattering from microbubbles were performed with both single elements transducers and a diagnostic ultrasound scanner. In general, PI has the most 2^{nd} harmonic without any 'nonlinear' fundamental, PM has mostly 'nonlinear fundamental, and PMPI has as much 'nonlinear' fundamental as PM and only slightly less 2^{nd} harmonic.

1 Introduction

Nonlinear acoustics and its application in biomedical ultrasound has been around for some time now. In the early 90s, harmonic imaging was developed for microbubble contrast agents; tissue was assumed to be linear. In fact, propagation of sound in body fluids and tissue is nonlinear and harmonics are also produced. In 1997, THI was introduced [1] and it is, since then, routinely used in diagnostic ultrasound imaging. Narrow bandwidths were originally used to prevent overlapping of the fundamental and harmonic components. Several pulsing schemes have been developed over the years to accommodate this problem and further improve the signal-to-noise ratio of harmonic imaging, with pulse inversion (PI) being the most common.[2-3]

Ultrasound contrast agents (UCAs) are used in cardiology for the assessment of myocardial perfusion and in radiology for the detection and characterization of tumours.[4] UCAs are also used for the characterization of atherosclerotic plaque in the carotid artery as well as the perfusion of the Vasa Vasorum which is considered a surrogate marker for the development of Cardiovascular Disease [5]. One widely used approach of imaging contrast agents is to use a low Mechanical Index (MI) nonlinear imaging technique to avoid bubble destruction and image both the macro– and micro–circulation in real-time. Nonlinear pulsing schemes are employed for the detection of nonlinear echoes from contrast microbubbles, and in addition to PI, power modulation [6], chirps [7], radial modulation [8-9] and many others are used.

The objective of this paper is to evaluate experimentally the various pulsing schemes for low MI imaging of contrast microbubbles and tissue harmonic imaging (nonlinear propagation) and better understand their similarities and differences. The pulsing schemes considered are pulse inversion, power modulation, and their combinations. In a previous work the same pulsing schemes were investigated with theoretical models and numerical simulations.[10] Now our work is expanded to include experimental data. Emphasis is placed on identifying whether nonlinearity due to propagation in tissue may be discriminated from nonlinearity due to scattering from bubbles. The relative harmonic levels in these schemes will be measured and analysed.

2 Materials and Methods

Pulsing schemes – Various pulsing schemes may be used to combine nonlinear responses from a system in a way that all linear (fundamental) energy is removed while certain nonlinear components are detected. The pulsing schemes investigated are described first. Whole and half amplitudes with phases of zero or π were considered. The various transmit amplitude coefficients, A_t and receive amplitude coefficients, A_r, are: (a) pulse inversion - PI, $[A_t(1, -1), A_r(1, 1)]$, (b) power modulation - PM, $[A_t (0.5, 1), A_r (2, -1)]$, (c) 2–state amplitude modulated pulse inversion - PMPI2, $[A_t (0.5, -1), A_r (2, 1)]$, and (d) 4–state amplitude modulated pulse inversion - PMPI4, $[A_t (0.5, -1, 1, -0.5), A_r (-2, -1, 1, 2)]$.

Every pulsing scheme was evaluated experimentally for nonlinear response detection in propagation in water and nonlinear scattering from resonant microbubbles (a numerical investigation has been reported before [10]). The receive amplitudes, A_r, may be scaled so that the summation of their absolute values equal one: $\Sigma|Ar| = 1$ to help with the comparisons between methods.

Experimental Setup - Up to 4 pulses were transmitted at a time, with relative amplitudes of 0.5, 1.0, -0.5 and -1.0. These pulses were designed in Arbitrary Express software by Tektronix, as a train of pulses. Each pulse was separated by 1ms thus being effectively equivalent to an imaging situation of a frame rate of 1000Hz. A Tektronix AFG3102 Arbitrary Function Generator was used to generate the train of pulses which was amplified by a 150A100B RF Amplifier by Amplifier Research. A Panametrics single element circular transducer transmitted the pulses which were received by a membrane hydrophone. Finally, a GPIB-USB2 interface was used to acquire the received pulses from the oscilloscope to a PC to be analyzed (see Fig. 1).

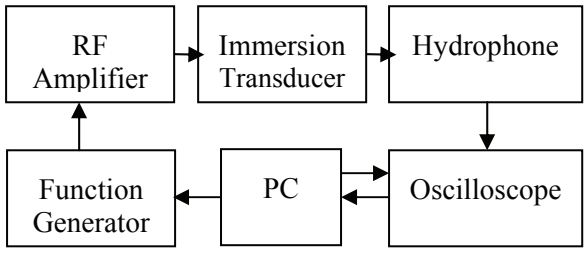

Fig.1 Block diagram for experimental setup.

The experiments were carried out in an ultrasonic tank filled with de-ionized water. A Newport micro-positioning system was used to align and control the position of the transducer and hydrophone. Three different experiments were carried out during this work: a) non-linear propagation in water, b) nonlinear scattering from ultrasound contrast agents (UCA) with single element transducers and c) nonlinear scattering from UCAs with a Phillips IU-22 C5-1 curve-linear array transducer.

In the nonlinear propagation experiment, a single element circular transducer was used to transmit the pulses to the focus, in de-ionized water, and a Precision Acoustics 0.4 mm element membrane hydrophone was used as a receiver. In the scattering experiments, shown in Fig.2, a specially designed container was used to hold the UCAs solution. The sides were made of thin mylar membrane to minimize reflections from the interface. The UCA was 0.1ml SonoVue (Bracco) diluted in 500 ml of de-ionized water. The amplitudes (proportional to the MI) used in microbubble experiments are very low to avoid bubble destruction. Another circular transducer was used as receiver, because of its higher sensitivity than a membrane or needle hydrophone. Finally, an IU-22 Philips ultrasound scanner was used for the last experiment where the same concentration of UCAS was insonified with a C5-1 convex array probe. The radio frequency (RF) data was collected from the scanner and analyzed with MatLab.

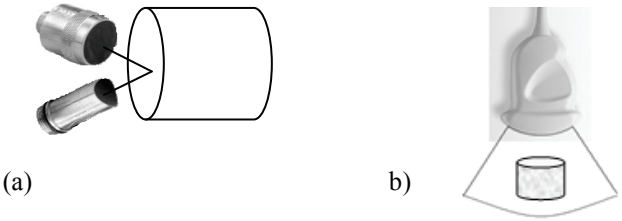

(a) b)

Fig. 2 Experimental set-up for scattering experiments: (a) with single element transducers, (b) with IU-22 and C5-1 convex array.

3 Results

Nonlinear propagation in water

Four unique pulses (with amplitudes of 0.5, 1.0, -0.5, -1.0) were propagated to the focus. In Fig.3, the waveforms and spectra of the four pulses are shown. For the spectra, the y-axis is dB-re 1MPa and the x-axis is in normalized frequency, f/f_o where 1 is the fundamental, 2 the 2nd harmonic etc. The spectra in Fig. 3 (b) and (f) are almost identical as the only difference is a π phase term. The same applies to the spectra of Fig. 3 (d) and (h). In a separate experiment we have found that the overall linear signal suppression of our system (function generator, power amplifier and transducer) is 40-43 dB for all pulsing schemes considered.

A wide range of nonlinear propagation experiments was carried out. Frequencies of 1 and 2.25 MHz and MIs from 0.1 to 2.5 and pulses with 2, 4 and 6 cycles were examined. A small selection of these experiments will be shown in this paper as they all follow similar trends. The pulses of Fig. 3 are used to produce the pulsing schemes of the second column of Fig. 4 (MI=1.7), where the other two columns correspond to MI=0.65 and MI=2.5.

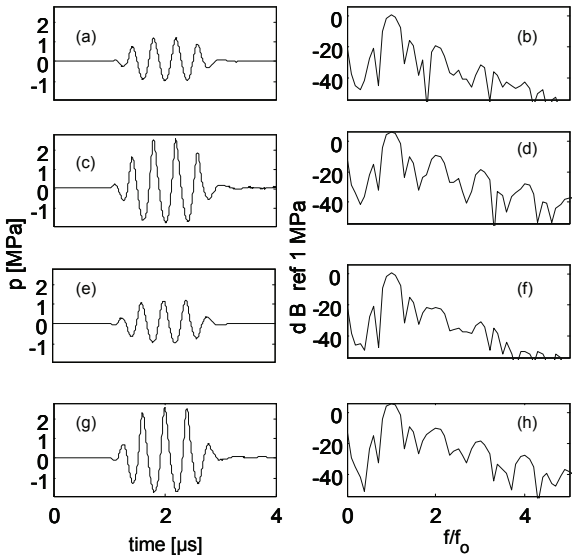

Fig.3 Waveforms and spectra of measurements of nonlinear propagation in water for the 4 amplitude and phase conditions considered in the various pulsing schemes.

Pulse inversion is shown in Fig. 4 (a)-(c). It is the result of adding the waveforms in Fig. 3(c) and (g). As noted earlier, the receive weights A_r are normalized such that the sum of their absolute values equals one [A_r(0.5, 0.5) for PI]. The resulting spectrum Fig. 4 (a)-(c) has only the even harmonic components (2nd and 4th). The 2nd and 4th harmonic components seen in the PI spectrum are *identical* with those shown in the spectra of either state (1 or -1) shown in Fig. 3(d) or (h).

Nonlinear propagation results for PM are shown in Fig. 4 (d)-(f). From the spectrum we see the resulting pulse has energy present in all harmonic components (1, 2, 3, 4). The energy shown in the spectrum is the result of nonlinear activity as it would be absent if a linear case was considered where the resulting pulse would be zero. By comparing Figs. 4 (b) and (e) we see that PI has a second harmonic that is 17 dB greater than that of PM (in the middle column, MI=1.7).

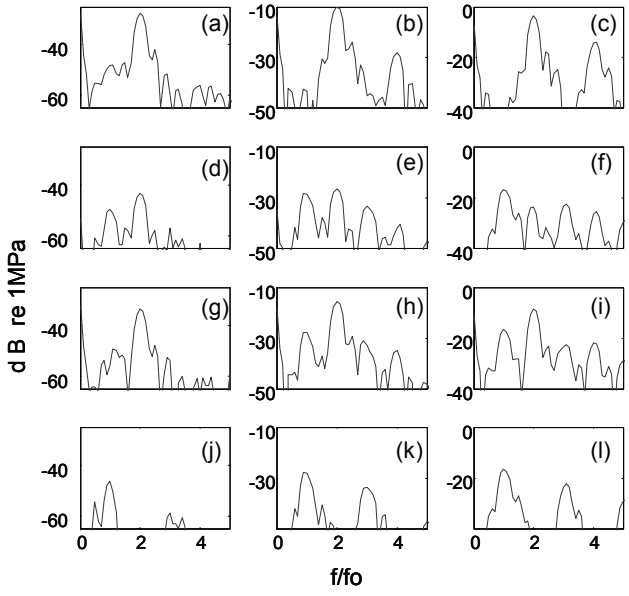

Fig.4 Nonlinear propagation with various pulsing schemes and various amplitudes. Comparison with theoretical results (a)-(c) PI, (d)-(f) PM, (g)-(i) PMPI2, (j)-(l) PMPI4. The different columns correspond to MI=0.65/1.7/2.5.

PMPI2 is considered in Fig. 4 (g)-(i). The resulting spectra are very similar to the PI spectra and with most energy on the 2nd harmonic. However, in Fig. 4(g)-(i) we also see both fundamental and third harmonic components not present in PI. Finally, the second harmonic of PMPI2 is 12 dB greater that of PM and 5 dB less than that of PI (in the middle column, MI=1.7).

PMPI4 is shown and in Fig. 4 (j)-(l). Most energy is present in the fundamental and third harmonic bands only. PMPI4 has small overall amplitude. A comparison of the nonlinear energy in the spectra of PMPI4 with one of the original transmitted pulses (0.5, 1, -0.5, -1) in Fig. 3, reveals that not all nonlinear energy of any of the harmonic components is present in the processed pulse.

Nonlinear scattering from microbubbles with single element transducers

In Fig. 5 the echoes from the four transmit pulses and their spectra after nonlinear scattering from microbubbles are shown. The transmit frequency is 1.2 MHz. In a similar fashion with the nonlinear propagation experiments in the previous section, the left column shows the individual bubble echoes from the individual pulses with amplitudes (0.5, 1, -0.5, -1) and the right column shows their respective spectra. In comparing the spectra in Fig. 3 with those in Fig. 5 we see that the bubble second harmonic relative to the fundamental is higher than the tissue propagation results despite the very low MI. This is expected as the bubble nonlinearity is higher than the nonlinearity created by propagation in water. The same applies to tissue nonlinearity when comparing propagation in tissue and scattering by microbubbles. As stated earlier, another circular single element transducer was used as receiver in this experiment. The reason is that with very low MIs to avoid bubble destruction the scattered sound has very small amplitude and the membrane hydrophone is not sensitive enough to detect such low signals. This however presents a drawback since the transducer has a limited bandwidth and thus capable to detect only the first two harmonic components. The transmitting transducer had a center frequency of 1.0 MHz but was used at 1.2MHz. The receiving transducer had a center frequency of 2.25MHz which was very close to the second harmonic of the transmit frequency.

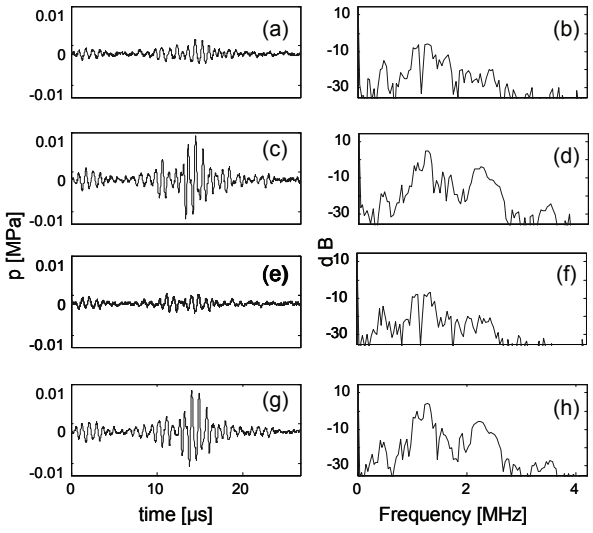

Fig.5 Nonlinear echoes and their spectra from UCAs using single element transducers for both transmit and receive.

It is noted that our spectra are not corrected for the frequency response of the receiver. Thus the second harmonic is shown at a higher relative level from the fundamental than it actually is.

Pulsing schemes for the echoes of Fig. 5 are shown in Fig. 6. In Fig. 6(a) and (b) results for PI are shown. The general trends are similar to the nonlinear propagation results, Fig. 4 (a)-(c), where only even harmonic components are preserved. However, it is noted that at the amplitudes used here for scattering from microbubbles are very low and the propagation in water (or tissue) is effectively linear. PM is considered in Fig. 6(c)-(d). The results here follow the same trends as in Fig 4 (d)-(f). A 'nonlinear' fundamental component and a second harmonic are seen in the spectra. Higher harmonics may not be seen due to the bandwidth of our receiver. The overall amplitude of PM is lower than that of PI as also seen in the nonlinear propagation results earlier. PMPI2 is shown in Fig. 6(e)-(f). In the spectrum Fig. 6(f) we see a slightly stronger than PM's second harmonic component, but also present are the fundamental and third harmonic identical in amplitude to those of PM. Comparing PI and PMPI2 we see that they both succeed in extracting second harmonic with PI having a slight edge in the overall signal level. PMPI4 is considered in Fig. 6(g)-(h). As we see in the spectrum Fig. 6(h) the fundamental and third harmonic (both in small amplitude) are present, with the second harmonic considerably lower than the level shown in PI, PM, and PMPI2.

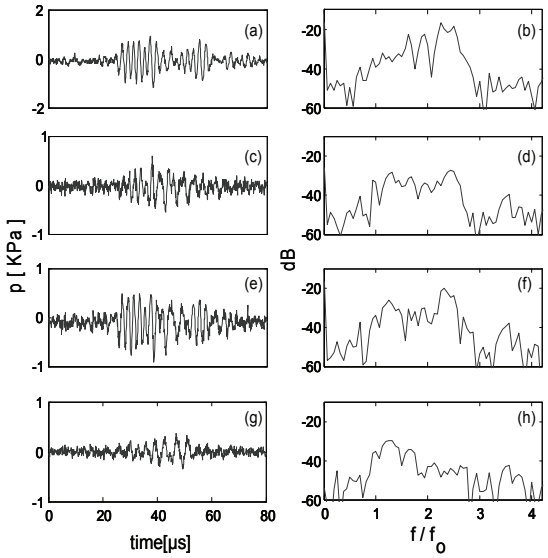

Fig.6 Nonlinear echoes with various pulsing schemes from UCAs using single element transducer.

Nonlinear scattering from microbubbles with iU-22

Experiments of nonlinear scattering from microbubbles were also performed with a diagnostic scanner Philips iU22 and a C5-1 curved linear array. We have measured the overall signal suppression of this system with the pulsing schemes and we have found it to be 32 dB, 47 dB, and 33 dB for PI, PM, and PMPI2, respectively. In Fig. 7(a) and (c) the two inverted pulses used in pulse inversion are shown. Their corresponding spectra are also shown in (b) and (d). Figure 7(e) shows the combination of the two pulses with receive coefficients [A_r (0.5, 0.5)]. A hamming window is applied to the received echoes as shown in Fig. 7(a). The fundamental component is suppressed by 35 dB whereas the second harmonic is fully detected. The

bandwidth of the C5-1 probe does not allow for the detection of the 4th harmonic. In Fig. 8 power modulation is presented. In PM, three pulses are transmitted down each ray line. One is a pulse transmitted by the odd components of the probe, one by the even, and one by the full aperture. As a consequence of linear diffraction, the even and odd components transmissions have half the amplitude of the full aperture transmission. The receive coefficients are [A_r (0.33, -0.33, 0.33)]. In Fig. 8 (a) and (c) microbubble echoes from the even element and full aperture transmissions are shown.

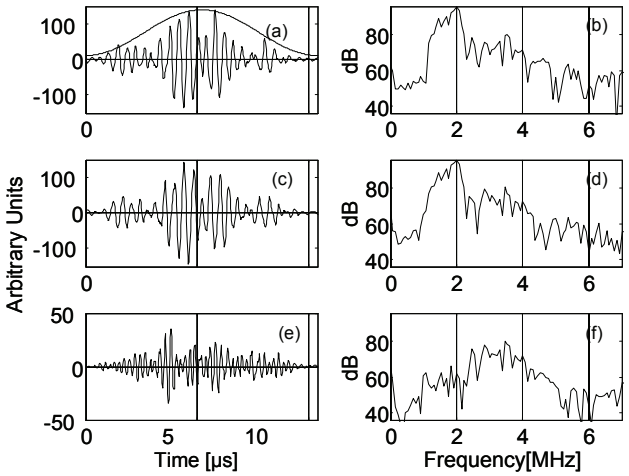

Fig.7 Radio frequency data from scattering from UCAs using IU-22 C5-1 curve-linear array transducer. (a)-(b) transmitted pulses, (c) PI (e)-(g) spectra.

Figure 8(e) shows the combination of the three pulses described above. The respective spectra are shown in Figs. (b), (d), (f). Figure 9 shows the results for PMPI2. The transmit sequence for PMPI2 is similar to PM except second full aperture pulse is also inverted and thus the receive coefficients are [A_r (0.33, 0.33, 0.33)]. In general, PI has the most 2nd harmonic without any 'nonlinear' fundamental, PM has mostly 'nonlinear fundamental, and PMPI has as much fundamental as PM and only slightly less 2nd harmonic.

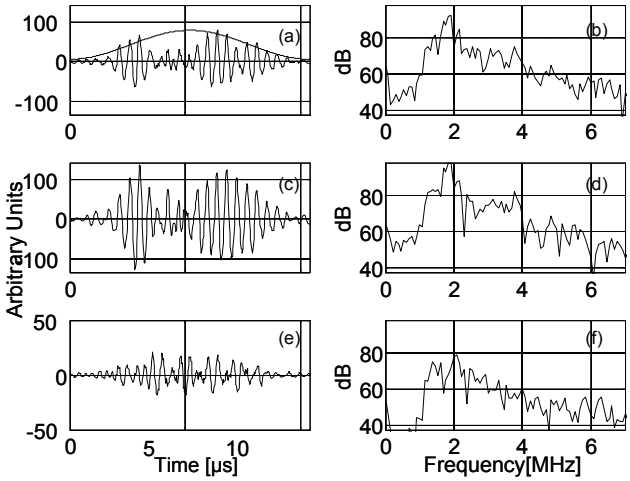

Fig.8 Radio frequency data from scattering from UCAs using IU-22 C5-1 curve-linear array transducer. (a)-(b) transmitted pulses, (c) PM, (e)-(g) spectra.

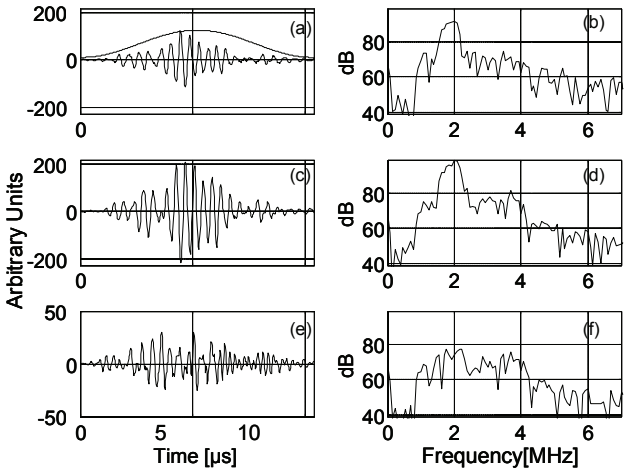

Fig.9 Radio frequency data from scattering from UCAs using IU-22 C5-1 curve-linear array transducer. (a)-(b) transmitted pulses, (c) PMPI, (e)-(g) spectra.

4 Discussion

An important observation is the similarity in terms of frequency content between the results for tissue nonlinearities and bubble nonlinearities. The general trends in Fig. 4 are similar to those in Figs. (6)-(9). It may be deduced from this observation that none of these techniques can identify what part of the nonlinear component is tissue versus bubbles. The one clear feature for discriminating between tissue and bubbles remains their difference in nonlinearity (bubbles are much more nonlinear than tissue). This is the main property that has been exploited in the past with low MI techniques. At very low MI (MI< 0.1), the nonlinear tissue response (nonlinear propagation) is much lower than that of microbubbles.

PI has the ability to fully extract even harmonics from nonlinear signals. As shown in Fig 10(a) the amplitude of the 2nd and 4th harmonic increases with increasing pressure until it reaches acoustic saturation. First and 3rd harmonics stay in the noise floor and this is expected as PI removes odd harmonics.

In PM, all harmonic components are present but not the full nonlinear response and we see this verified in Fig 10(b). All harmonic components increase with increasing amplitude only limited with acoustic saturation (increasing the source pressure results in producing higher harmonics). We note that the 2nd harmonic starts to decrease at high pressures. PMPI2 follows the same trends as PM with the second harmonic being considerably higher than that of PM. The other components (1st and 3rd) are identical between PM and PMPI2. PMPI4 was the ability to extract odd harmonics and this is verified by Fig 10(d). These components (1st and 3rd) are identical to those in PM and PMPI2.

The 'nonlinear' fundamental is the result of using two unequal amplitudes and looking at their differential response. The nonlinear systems discussed here do not generate any nonlinear energy in the fundamental band. What is seen in the fundamental band is the difference in the scaled linear responses after some energy was moved in the higher harmonics as a result of nonlinear activity.

Finally we note that the 'nonlinear' fundamental becomes important in tissue imaging because it suffers less attenuation than the 2nd harmonic especially in cases where sensitivity is compromised due to absorption losses.

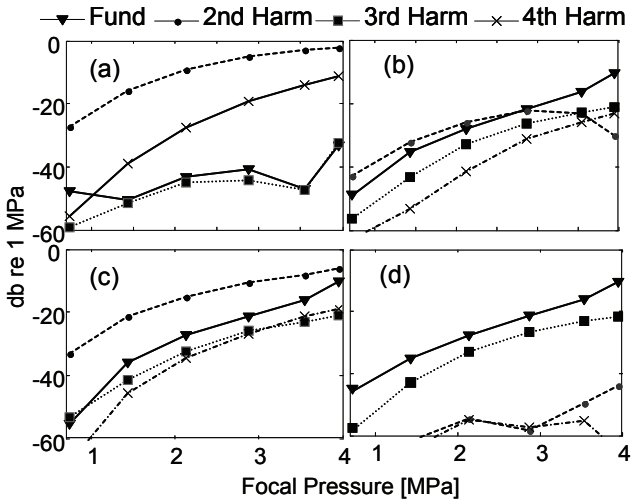

Fig. 10 Trends of the various harmonics (a) PI, (b) PM, (c) PMPI2, (d) PMPI4

5 Conclusion

We have verified experimentally in nonlinear propagation in water and in scattering from microbubbles that the pulsing schemes considered isolate various nonlinear components and remove all linear response. Our measurements are in close agreement with previously reported theoretical investigation by some of the present authors.[10]

PI uses two identical inputs that only differ in phase and it *isolates* the even harmonic components. With PI we get the total amount of nonlinearity present in those components only (even harmonics). In addition, for low nonlinearity (quassi-linear case) where only fundamental and second harmonics are present, the second harmonic is the total amount of nonlinear energy. With pulsing schemes where different amplitudes are used (PM), we are forced to look at the *differential* nonlinearity between the 2 or more states of input. In the limiting case where one pulse is at full amplitude and the other is almost at zero (or zero nonlinearity), their difference would then result in the *total* nonlinearity. With two or more states at full and half amplitudes the resulting pulse will have less nonlinear energy than the full amplitude result (A_t=1).

Acknowledgments

This work is supported by the *Cyprus Research Promotion Foundation* though the grant *Vasorum* (Grant number: *Ygeia/0506/06*).

References

[1] M. A. Averkiou, D. N. Roundhill, and J. E. Powers, "A new imaging technique based on the nonlinear properties of tissues*," in Proceedings of the 1997 IEEE Ultrasonics Symposium*, Toronto, Canada, vol. 2, 1561-1566, 1997.

[2] D. H. Simpson, C. T. Chen, P. N. Burns, "Pulse inversion Doppler: a new method for detecting nonlinear echoes from microbubble contrast agents," *IEEE Trans Ultrason Ferroelect, Freq Contr.*, **46**:372–382, 1999.

[3] M. Averkiou, "Tissue harmonic ultrasonic imaging," in Optical and acoustical imaging of biological media, C. R. Acad. Sci. Paris, Applied Physics(Biophysiscs), t. 2, Serie IV, Elsevier, Paris, pp.1139-1151, 2001.

[4] M. Bruce, M. A. Averkiou, K. Tiemann, J. Powers, and K. Beech, "Vascular flow and perfusion imaging with ultrasound contrast agents," Ultrasound in Med. & Biol. 30(6), 735-743, 2004.

[5] E. Vicenzini et al, "Detection of carotid adventitial vasa vasorum and plaque vascularization with ultrasound cadence contrast pulse sequencing technique and echo-contrast agent," Stroke, vol. 38, number 10, pp. 2841-2843, 2007.

[6] M. Averkiou, J. Powers, D. Skyba, M. Bruce, and S. Jensen, "Ultrasound contrast imaging research," *Ultrasound Quarterly*, **19**(1), 27-37, 2003.

[7] J. M. Borsboom, C. T. Chin, A. Bouakaz, M. Versluis, and N. de Jong, "Harmonic Chirp Imaging Method for Ultrasound Contrast Agent," *IEEE Trans Ultrason Ferroelect, Freq Contr.*, **54:11**:2283–2290, 2007.

[8] A. Bouakaz, M. Versluis, J. Borsboom, and N. de Jong, "Radial Modulation of Microbubbles for Ultrasound Contrast Imaging," *IEEE Trans Ultrason Ferroelect, Freq Contr.*, **52:2**:241–249, 2005.

[9] B. A. Angelsen and R. Hansen, "SURF Imaging - A New Method for Ultrasound Contrast Agent Imaging," *," in Proceedings of the 2007 IEEE Ultrasonics Symposium*, New York, USA, 531-541, 2007.

[10] M. A. Averkiou, M. Bruce, S. Jensen, P. Rafter, T. Brock-Fisher, and J. Powers, "Pulsing schemes for the detection of nonlinear echoes from contrast microbubbles," *in Proceedings of the 9th European Symposium on Ultrasound Contrast Imaging*, Rotterdam, The Netherlands, pp.17-24, Jan. 2004.